We are IntechOpen, the world's leading publisher of Open Access books Built by scientists, for scientists

4,800
Open access books available

122,000
International authors and editors

135M
Downloads

154
Countries delivered to

Our authors are among the

TOP 1%
most cited scientists

12.2%
Contributors from top 500 universities

CLARIVATE ANALYTICS
BOOK CITATION INDEX
INDEXED

WEB OF SCIENCE™

Selection of our books indexed in the Book Citation Index
in Web of Science™ Core Collection (BKCI)

Interested in publishing with us?
Contact book.department@intechopen.com

High Temperature Creep of Metal Oxides

Krystyna Schneider and Mieczyslaw Rekas

Additional information is available at the end of the chapter

Abstract

This chapter presents a comprehensive review of the creep technique used for the study of defect structure and diffusion in metal oxides, both single crystals and ceramics. At high temperatures, the creep rate is proportional to the diffusion coefficient of the slowest species in solid compounds, whatever deformation mechanisms are present (Nabarro viscous creep, recovery creep or pure climb creep). The creep rate dependence on deviation from stoichiometry can be determined from this diffusion. In the case of metal oxides, the departure from stoichiometry is controlled by the oxygen activity which usually is identified with oxygen partial pressure, p_{O_2}. The p_{O_2} dependence of the creep rate provides direct information about the nature of minority point defects. On the other hand, studies of the temperature dependency of the creep rate inform us about the activation energy of the diffusion coefficient. This review focuses primarily on the creep behavior of transition metal oxides such as $Ni_{1-y}O$, $Co_{1-y}O$, $Fe_{1-y}O$ exhibiting disorder in metal sublattice, as well as ZrO_{2-x} with majority defects in oxygen sublattice. The advantage of these studies is determination of both defect structure and diffusion coefficients of minority defects namely in oxygen sublattice in iron-triad oxides and in zirconium ZrO_2 sublattice.

Keywords: high temperature creep of metal oxides, defect structure, nonstoichiometry, diffusion

1. Introduction

This chapter presents a review of the creep technique used for the study of defect structure and diffusion in metal oxides. Transition metals of the iron-row triad (Fe, Co, Ni) monoxides were chosen. These oxides at higher temperatures exhibit electronic conductivity. Zirconia stabilized with yttria, termed as YSZ, was also the subject of interest. This material is treated as model system of ionic (super ionic) conductor. Taking into account that creep behavior of the oxides is generally dependent of the minority defects properties (types and concentrations) which are

especially strictly related with majority point defect, a short description of the point defect structure of each analyzed oxide proceeds the appropriate chapter.

2. Definition of terms

Creep, or more generally high-temperature plastic deformation of metal oxides, is a suitable method for measuring diffusion coefficients and to assess the nature of point defects responsible for diffusion processes. Above a so called Tamman's temperature and under constant applied stress, a steady state is reached where the rate of deformation remains constant. Tamman's temperature of metal oxides assumes value of about $0.45 \times T_{melt}$ [K] [1] creep rates, $\dot{\varepsilon}$, is commonly expressed by the equation [2]

$$\dot{\varepsilon} = \frac{d\varepsilon}{dt} = \frac{A\sigma^m}{d^b} exp\left[-\frac{Q}{kT}\right] \qquad (1)$$

where ε is the creep strain, A is constant dependent of the material structure and the creep mechanism, σ is the applied stress, m and b are exponents dependent on the creep mechanism, d is the grain diameter, k is Boltzmann's constant, T is the absolute temperature and Q is an activation energy of the creep.

At high temperatures, the creep rate is proportional to some diffusion coefficient, whatever the exact nature of deformation mechanism: Nabarro-Hearing creep, grain boundary sliding and dislocation movements are valid [3]. This diffusion coefficient, D, is an effective diffusivity involving both the lattice and the grain boundaries diffusivities. In most cases, it reduces to the diffusivity of the slowest species. In case of transition metal oxides, the creep rate dependence on deviation from stoichiometry is carried out through diffusivity. In binary oxides, at high temperatures the deviation from stoichiometry and related majority point defects are controlled by the oxygen partial pressure, p_{O_2}. In most cases, these defects are only located either in metal or oxygen sublattice. Defects on other sublattice are present in a much lower concentration (named as 'minority defects'), and the diffusivity of the corresponding species is very low. Their diffusion coefficient is proportional to the concentration of minority defects, which also varies as some characteristic power law with p_{O_2}, so that creep rate has related to this variable. Accordingly, the p_{O_2} dependence of the creep rate leads to a direct approach to assess the nature of the minority point defects [2]

$$\dot{\varepsilon} = \frac{d\varepsilon}{dt} = \frac{C\sigma^m}{d^b} p_{O_2}^{\frac{1}{n}} exp\left[-\frac{E_{act}}{kT}\right] \qquad (2)$$

where $C = Ap_{O_2}^{-\frac{1}{n}}$, $E_{act} = Q$ is the energy activation of diffusion and n is the parameter dependent of the point defect structure.

3. Creep of transition metal monoxides

The transition metal monoxides such as iron-triad group (Fe, Co, Ni) show only metal deficiency: $Fe_{1-y}O$, $Co_{1-y}O$ and $Ni_{1-y}O$. The nonstoichiometry and related point defect structure discussed below for these oxides are based on both thermogravimetric equilibration and electrochemical measurements. The nonstoichiometry, y, is most pronounced with $Fe_{1-y}O$ (y = 0.043−0.167) [4, 5], whereas in $Co_{1-y}O$ [6] and $Ni_{1-y}O$ [7] y is about 0.000–0.012 and 0.0000–0.0010, respectively.

Nonstoichiometry y in $M_{1-y}O$ (M = Fe, Co, Ni) can be modified by changes of oxygen activity, p_{O_2}, in thermodynamic equilibrium with the oxide crystal (Kröger and Vink [8] notation of defects is used throughout this paper):

$$\frac{1}{2}O_2 \Leftrightarrow V_M^{i-} + ih^\bullet + O_O \tag{3}$$

where i = 0, 1, 2 denotes the degree ionization. The nonstoichiometry of the $M_{1-y}O$ is then given by:

$$y = \left[V_M^x\right] + \left[V_M'\right] + \left[V_M''\right] \tag{4}$$

Applying the mass action law to reaction (3) and assuming that interaction among defects may be neglected, as well as supposing appropriate electroneutrality conditions, one arrives at the following relationship between nonstoichiometry and equilibrium oxygen pressure and temperature:

$$y = y_o p_{O_2}^{1/n_y} \exp\left(-\frac{E_y}{RT}\right) \tag{5}$$

where $1/n_y$, or simply n_y, is the parameter depending on the ionization degree of cation vacancies, assuming 2, 4 and 6 values for neutral, single- and double-ionized vacancies, respectively; E_y denotes the temperature coefficient directly related to the enthalpy of defect formation.

$M_{1-y}O$ (M = Fe, Co, Ni) are p-type semiconductors, which electrical conductivity is realized by electron (or electron hole) hopping mechanism between M^{3+} and M^{2+} ions. The concentration of quasi-free electron holes $[h^\bullet]$ is given by:

$$[h^\bullet] = \left[V_M'\right] + 2\left[V_M''\right] \tag{6}$$

Accordingly, the following relationship between electrical conductivity, σ and equilibrium oxygen pressure and temperature is given by:

$$\sigma = e\mu_h[h^\bullet] = \sigma^o \, p_{O_2}^{1/n_\sigma} \exp\left(-\frac{E_\sigma}{RT}\right) \tag{7a}$$

or

$$[h^{\bullet}] = h^o \left(p_{O_2}\right)^{\frac{1}{n_{\sigma}}} \exp\left(-\frac{E_{\sigma}}{RT}\right) \tag{7b}$$

where e is the elementary charge, μ is mobility of the holes, σ^o and h^o are constants involving mobility of electron holes and entropy terms of the equilibrium constant of the reaction (3), n_{σ} is the parameter depending on the ionization degree of cation vacancies, assuming ∝, 4 and 6 values for neutral, single- and double-ionized vacancies, respectively; E_{σ} denotes the activation energy of the electrical conductivity.

Several minority defects can be proposed in $M_{1-y}O$. Considering only simple defects oxygen vacancies V_O^{j+} (j = 1 or 2) or oxygen interstitials O_i^{k-} (k = 1 or 2) the formation of these defects is described by the following:

$$O_O + j\, h^{\bullet} \Leftrightarrow V_O^{j+} + \frac{1}{2}O_2 \tag{8}$$

and

$$\frac{1}{2}O_2 \Leftrightarrow O_i^{k-} + k\, h^{\bullet} \tag{9}$$

Applying the mass action law to these equilibriums and taking into account the Eq. (7b), we can write the following relationships:

$$\left[V_O^{j+}\right] = K_j^o (h^o)^j \left(p_{O_2}\right)^{\left(\frac{j}{n_{\sigma}} - \frac{1}{2}\right)} \exp\left[\frac{-jE_{\sigma} + \Delta H_j)}{RT}\right] \tag{10}$$

and

$$\left[O_i^{k-}\right] = K_i^o (h^o)^{-k} \left(p_{O_2}\right)^{\left(\frac{1}{2} - \frac{k}{n_{\sigma}}\right)} \exp\left[\frac{-\Delta H_k - kE_{\sigma})}{RT}\right] \tag{11}$$

From Eqs. (2) and (10),

$$\frac{1}{n} = \frac{j}{n_{\sigma}} - \frac{1}{2} \tag{12}$$

and

$$E_{act} = jE_{\sigma} + \Delta H_j \tag{13}$$

Similarly, from Eqs. (2) and (11),

$$\frac{1}{n} = \frac{1}{2} - \frac{k}{n_{\sigma}} \tag{14}$$

and

$$E_{act} = \Delta H_k - kE_\sigma \qquad (15)$$

So, using Eqs. (12) and (13) or Eqs. (14) and (15) carrying out the creep rates measurements as a function of oxygen partial pressure and temperature, we can determine both parameters n and E_{act}. Then, using the values of electrical properties such as electrical conductivity (or Seebeck coefficient) which are related to the concentration of the electron holes, we can identify the type of minority defect responsible for the creep diffusion process and can determine the activation energy of the diffusion.

3.1. Creep of NiO

Nickel oxide is a nonstoichiometric compound with a deficit of metal. Its chemical formula may be written as $Ni_{1-y}O$. The resulting majority point defects are nickel vacancies formula may be written as $Ni_{1-y}O$. The resulting majority point defects are nickel vacancies: V_{Ni}', V_{Ni}'' and electron holes (**Figure 1**) [7]. The dependence of electrical conductivity, σ, as a function of oxygen partial pressure, p_{O_2} and temperature is shown in **Figure 2** [9, 10]. The reciprocal of oxygen exponent $n_\sigma = n_h$ varies values between 4 and 6.

The results of the creep studies of NiO single crystals [11, 12] and NiO polycrystals [3, 13, 14] are summarized in **Table 1**. The comparison of the activation energies for creep rate with oxygen self-diffusion obtained by Dubois et al. [15, 16] agrees only with a rather large uncertainty [17–19]. Controversy, **Figure 3** presents the diffusion coefficients determined by tracer of nickel [17, 18] and by the tracer self-diffusion of oxygen [19] on one hand, and the diffusion coefficient determined using the creep technique, on the other. The excellent agreement is observed between oxygen diffusion coefficient and the diffusion coefficient from the creep.
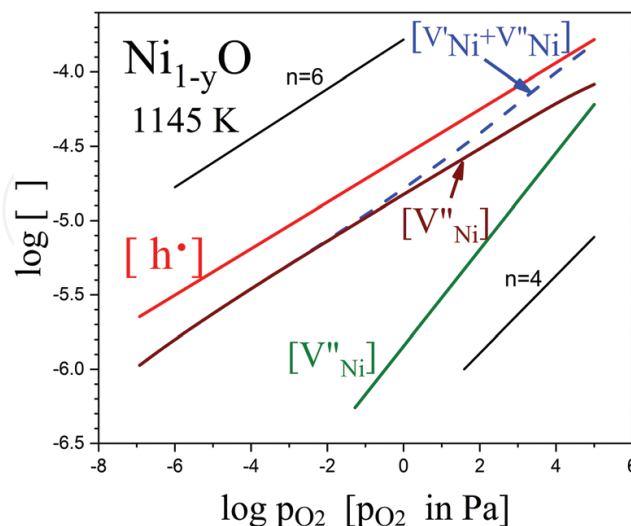
Figure 1. Majority defect concentration in $Ni_{1-y}O$. Defect concentrations ([ ]) are unitless values. They are expressed as Ni-site ratio.
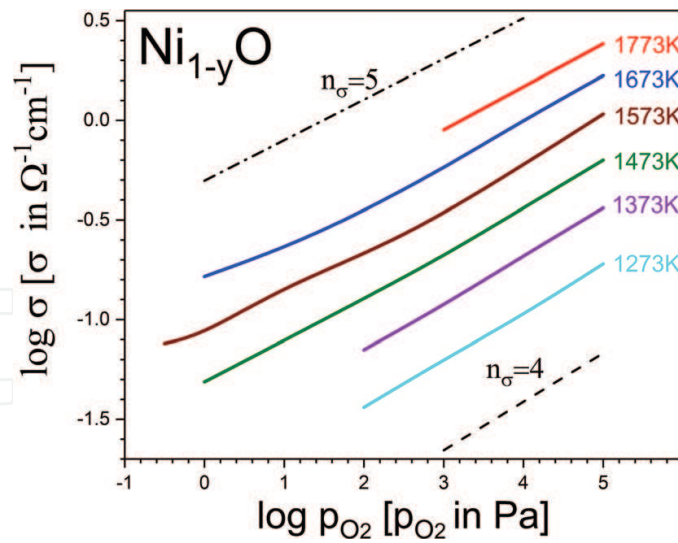
Figure 2. Electrical conductivity of at 1145 K Ni$_{1-y}$O [9, 10].

Material	T/T$_m$**	σ (MPa)	p$_{O_2}$ (Pa)	m	E$_{act}$ (eV)	n	Minority defect	Mechanism of creep	Ref.
NiO s.crystal	0.09–0.66	20–100	0.1–2 × 10⁴	NA	NA	NA	NA	NA	[11]
NiO s.crystal	0.6–0.8	15–120	1–2 × 10⁴	12 7	5.4–8.5	−0.06 to +0.11	V$_O^{••}$	Thermally activated glide recovery creep	[12]
NiO polycrytals	0.6–0.8	6–20 20–90 90	1–2 × 10⁴	1.5 7.9	3.8	0–0.03	V$_O^{••}$	Nabarro creep	[13]
NiO polycrystals	0.56–0.61	34.5–79.8	2 × 10⁴	3.25 ± 0.18	2.46 ± 0.31	NA	NA	Diffusion controlled climb glide	[25]
CoO s.crystal	0.49–0.66	6.9–31	2.1 × 10⁴ 1.1 × 10⁻⁴	4.6 3.3	2.9 1.77	NA	NA	Diffusion	[24]
CoO s.crystal	0.61–0.75	8.3–14.5	NA	5	2.2	NA	NA	Diffusion controlled dislocation motion	[25]
CoO s.crystal	0.61–0.80	2–20	10⁻⁶ 1 × 10⁵	4.4–5.6	3.1–4.7	2	V$_O^{••}$ \ O$_i^x$, O$_i^-$ O$_i^{2-}$	Oxygen diffusion	[26]
CoO s.crystal	0.6 0.8	5–25	1 2 × 10⁴	8.5 6.5	5 2.5–5	0.5 0.1	O$_i^{''}$ V$_O^{••}$	Oxygen diffusion	[27]
CoiO polycrytals	0.58–0.62	34.5–79.8	2 × 10⁴	3	3.12	NA	Na	Dislocation motion	[14]
FeO polycrystals	0.73–0.95	2.5–15	10⁻¹⁰–3 × 10⁻⁸	4.15 ± 0.10	2.8	NA	V$_O^{••}$	Climbing dislocations	[37]
FeO s.crystal	0.67 0.85	3.2–5.3	3 × 10⁻¹³–2 × 10⁻⁶	5.3 4.2	3.0 ± 0.4	−0.015 +0.11	O$_i^{''}$ O$_i^{'}$	Diffusion controlled recovery	[38]

*Denotation of symbols, see Eq. (2).

**T$_m$ – Melting temperature (K).

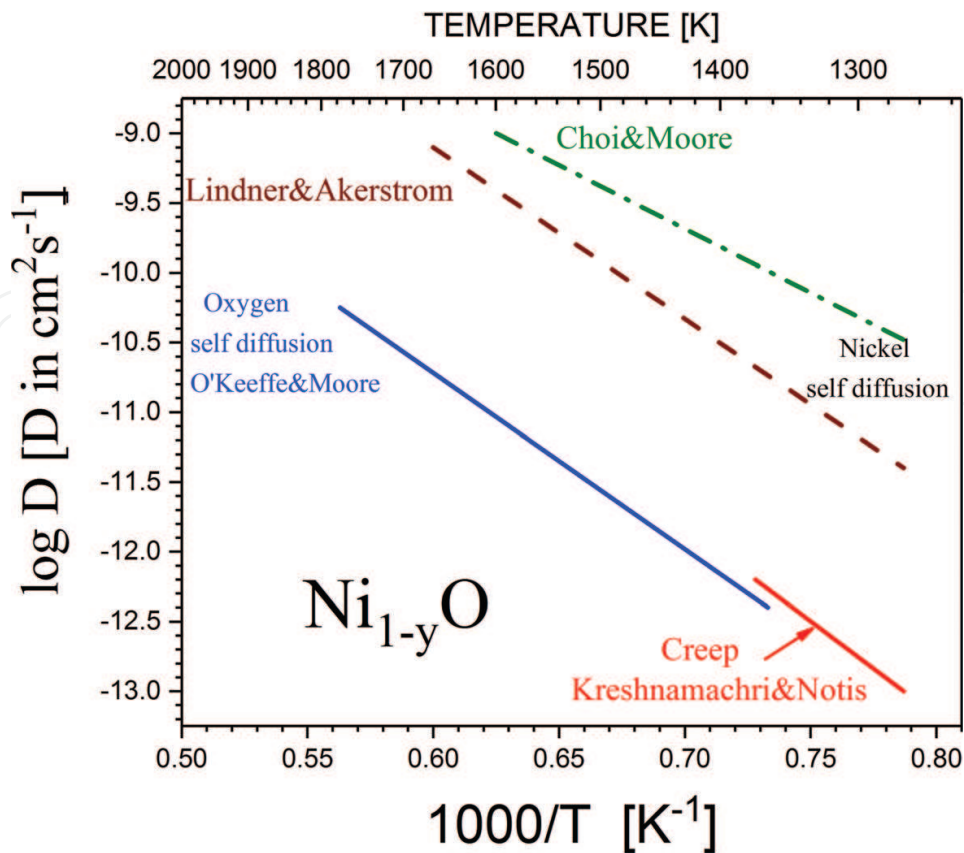**Table 1.** Creep results of NiO, CoO and FeO*.

Figure 3. Temperature dependence of diffusion coefficients [14, 17–19].

3.2. Creep of CoO

Taking into account both crystal structure and nonstoichiometry departure, CoO shows similarities to NiO. However, there is a major difference at low temperature (below 1170 K) and high oxygen pressure CoO is unstable and transforms to the spinel-type Co_3O_4 (**Figure 4**). Also the departure of stoichiometry, y, in $Co_{1-y}O$ is about 10 times higher than that of $Ni_{1-y}O$. Traditional analysis of point defect structure in $Co_{1-y}O$ based on the ideal defect model with the assumption that point defects in $Co_{1-y}O$ are randomly distributed and do not interact with each other, leads to the conclusion that at high p_{O_2} (close to CoO/Co_3O_4 border) the predominant ionic point defects are V_{Co}^x and V_{Co}'; at the intermediate region of p_{O_2} both V_{Co}' and V_{Co}'' coexist together as the predominant ionic point defects; and finally near the border Co/CoO the doubly ionized cobalt vacancies V_{Co}'' are predominant [20]. However, the assumption of validity of ideal point defects in CoO is questionable. The ideal point defect model gives satisfactory results when nonstoichiometry departure and related point defect concentration is below 0.1 at%, for higher concentrations interaction between defects must be taken into account [21].

The interaction between defects in $Co_{1-y}O$ can be well described by the Debye-Hückel approach [22]. In addition, the model proposed is based on the assumption that the only type of predominant ionic defects present in cobalt monoxide at elevated temperatures are double-ionized cation vacancies, V_{Co}'' instead of two or even more types of ionic defects considered before. Despite the simplicity of the model, the agreement with the experiment is very good within the entire range of CoO stability.
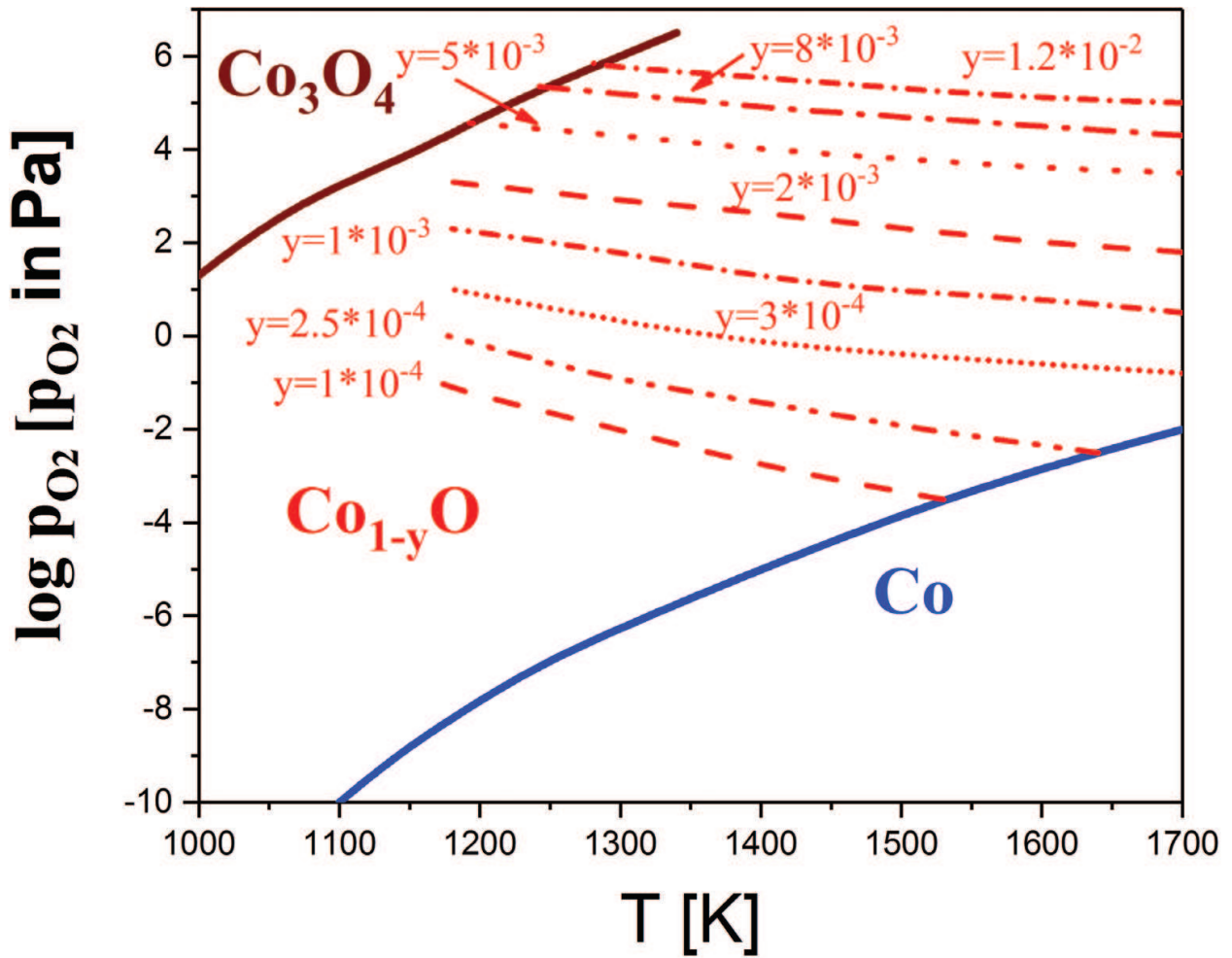
Figure 4. Stability range of $Co_{1-y}O$ [6, 20].

Apart from the Debye-Hückel model, there is also another model making allowance for interaction between the defects which explains well the experimental data of CoO, in particular at high values of deviation from stoichiometric composition (i.e. close to the $Co_{1-y}O/Co_3O_4$. This so called cluster model involves the formation of 4:1 clusters consisting of four double-ionized octahedral cobalt vacancies and one trivalent Co ion in tetrahedral interstitial position: $[(V_{Co})_4Co_i]^{3-}$ [23]. **Figure 5** [20] shows the plots of electrical conductivity, σ, as a function of oxygen partial pressure and temperature. The dependences shown can be used to determine the reciprocal of oxygen exponent $n_\sigma = n_h$ defined in Eq. (7a). The exact value of n_h is needed in the interpretation of the creep rate versus p_{O_2}.

The results of the creep studies of CoO single crystals [24–28] and CoO polycrystals [14] are summarized in **Table 1**. A comparison of the activation energies for creep rate with oxygen self-diffusion obtained by Dubois et al. [15, 16] agrees only with a rather large uncertainty.
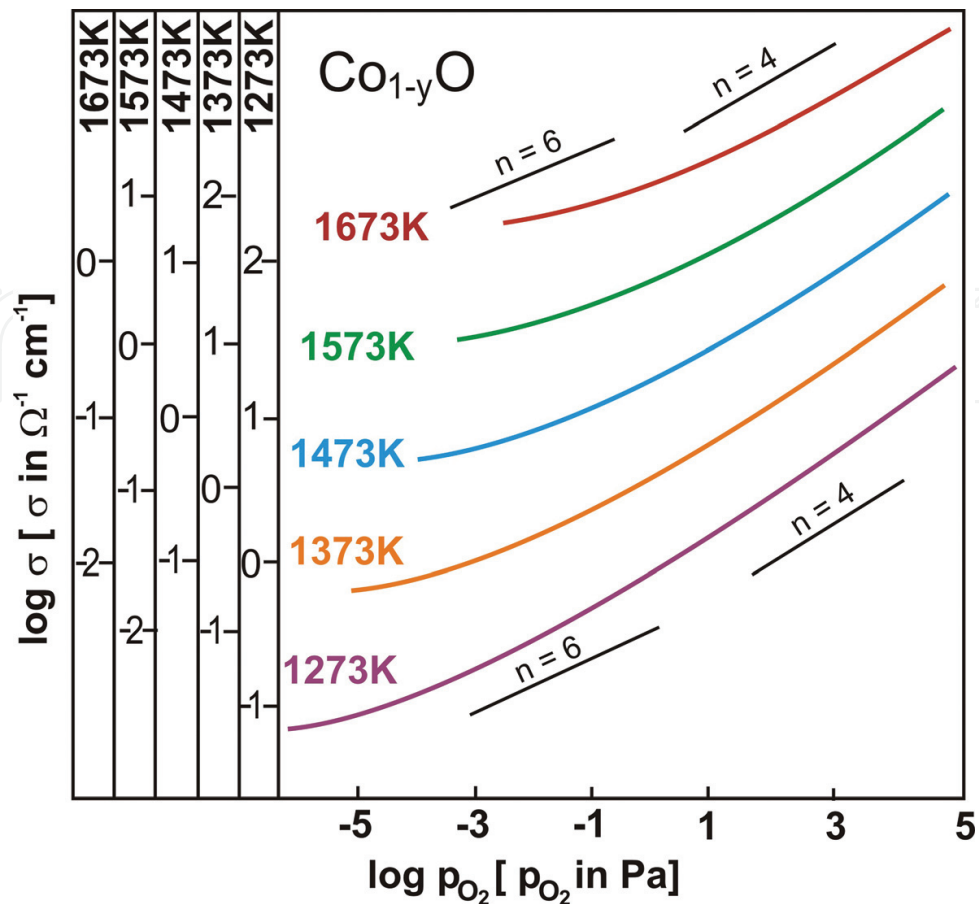
Figure 5. Electrical conductivity, σ, as a function oxygen partial pressure and temperature [20].

3.3. Creep of FeO

Iron monoxide, termed also as wüstite, has the NaCl-type structure. Compared to other binary oxides of iron-row metals, the wüstite phase exhibits the highest deviation from stoichiometry, varying from 4.3 at% at the $Fe/Fe_{1-y}O$ phase boundary up to 16.7 at% at the $Fe_{1-y}O/Fe_3O_4$ interphase (**Figure 6**) [4, 5, 29]. The non-stoichiometry occurs because of the ease of oxidation of Fe^{2+} to Fe^{3+} effectively replacing a small portion of Fe^{2+} with two-thirds their number of Fe^{3+}, which take up tetrahedral positions in the close packed oxide lattice. The considerable concentration of defects, resulting from nonstoichiometry, leads to their strong interactions and formation of complexes. On the basis of neutron diffraction studies, Roth [30] has proposed the formation of defect complexes composed of two iron vacancies and interstitial iron $\left[(V_{Fe}'')_2 Fe_i^{3+} \right]'$. This defect is similar to an element of the spinel structure of magnetite Fe_3O_4. Therefore, the Roth complexes can be formally considered as a magnetite-type defect or a submicrodomain of Fe_3O_4 in FeO [28, 31]. On the basis of X-ray studies, Koch and Cohen [32] have postulated that defects in $Fe_{1-y}O$ form associates even larger than Roth 2:1 complexes, composed of 13 iron vacancies and 4 interstitials (termed as cluster 13:4). The formation of the clusters was later confirmed by the neutron diffraction
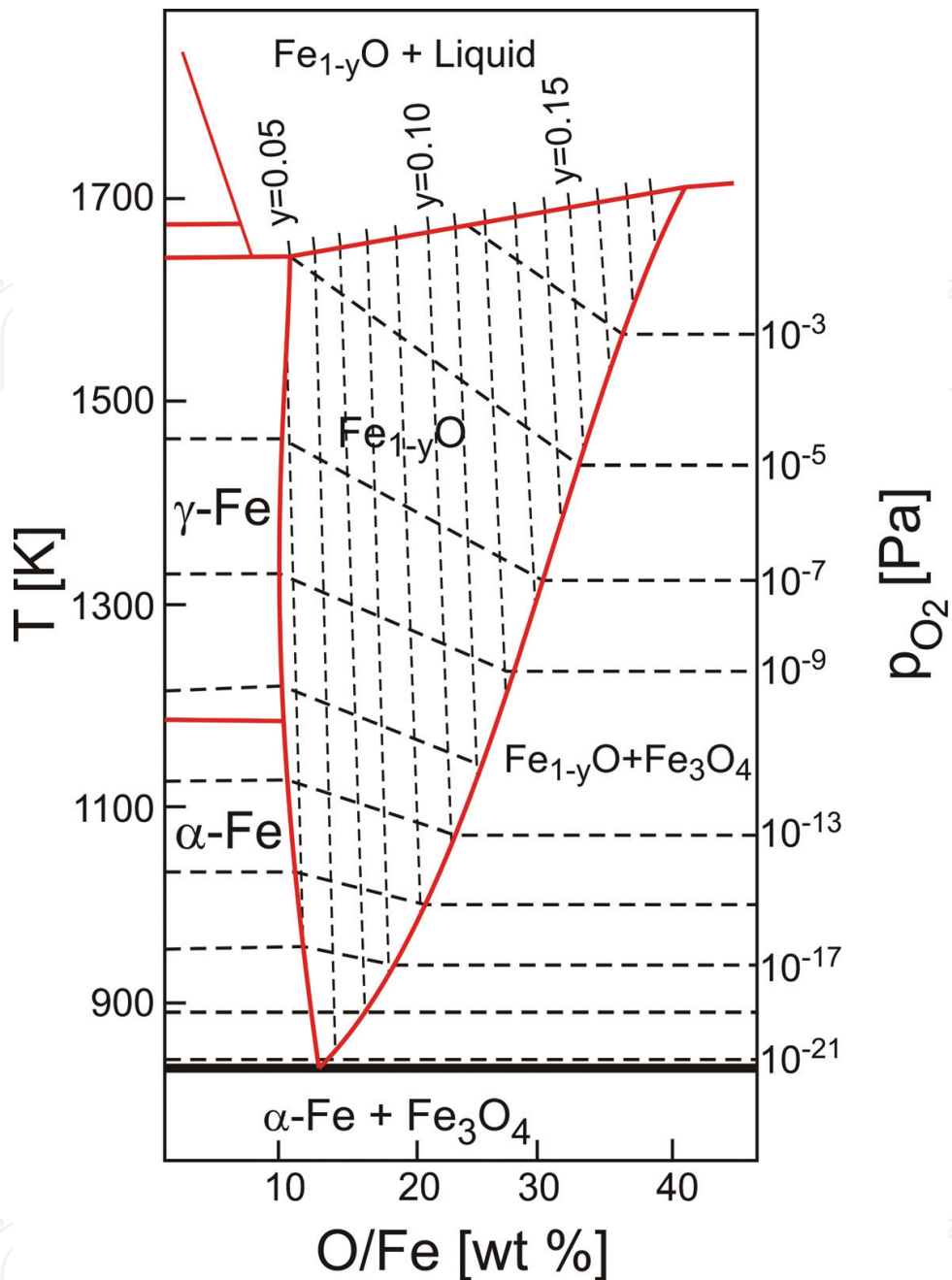
Figure 6. Stability range of Feo$_{1-y}$O [4, 5, 29].

studies of Cheetham et al. [33, 34]. Catlow et al. [35, 36] using the computer simulation method have proposed various kinds of defect clusters such as 4:1, 6:2. 8:3, 10:4, 12:4 and 16:5. It has been postulated that the 4:1 cluster is a constructional unit in formation of higher order clusters. The cluster 16:5 resembles the magnetite structure and can be considered as a Fe$_3$O$_4$-type microdefect.

The creep studies of FeO single crystals were performed by Ilschner et al. [37] and by Jolles and Monty [38]. The required parameter $n_h = n = \frac{e}{k} \left[\frac{\partial \alpha}{\partial \ln p_{O_2}} \right]^{-1}$ (where α is Seebeck coefficient) needed

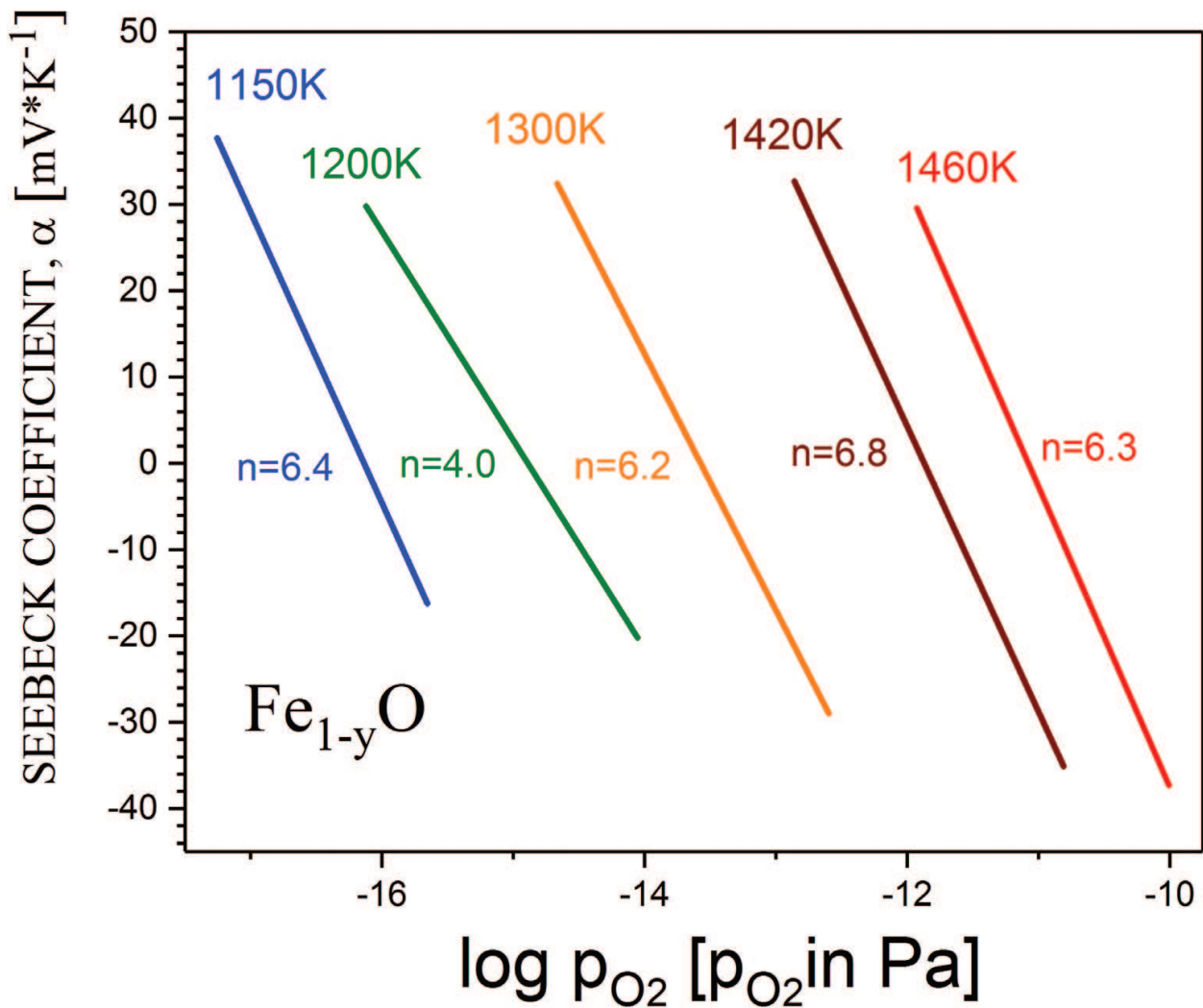**Figure 7.** Seebeck coefficient, α, of $Fe_{1-y}O$ [31].

to interpretation of the creep rate versus p_{O_2} is presented in **Figure 7**. The results of the creep studies are summarized in **Table 1**.

4. Zirconia-based materials

Zirconium dioxide, ZrO_2 has three polymorphic modifications: monoclinic below 1440 K, tetragonal 1440–2640 K and cubic above 2640 K. The transition between them involves a large volume expansion cause a cracking upon cooling from high temperature, which is detrimental to the materials structural applications. The destructive phase transformation can be suppressed by total or partial stabilization of high temperature modifications (cubic or tetragonal form). This stabilization consists on the addition to ZrO_2 several mole % of MgO, CaO or Y_2O_3 among others. The most popular stabilizer is Y_2O_3 termed as yttria.

Yttria-stabilized zirconia (YSZ) ceramics is a strategic functional material which has found extensive applications in electrochemical devices, such as gas sensors, solid oxide fuel cells and electrolysis cells.

Also the YSZ well known as an excellent construction material due to such properties as: high hardness, low wear resistance, low coefficient of friction, high elastic modules, chemical inertness, low thermal conductivity and high melting point [39–42]. It is also recognized that the useful mechanical properties are obtained in multiphase material known as partially stabilized zirconia (PSZ). Garvie and Nicholson [43] have demonstrated that a fine-scale precipitate of monoclinic zirconia in a cubic stabilized matrix enhances the strength of PSZ. Very interested mechanical properties were discovered in fine-grained tetragonal ZrO_2 stabilized with 3 mol% Y_2O_3 termed as 3Y-TZP [44, 45]. The macroscopic and microscopic behavior of 3Y-TZP can be characterized as structural or micrograin superplasticity, according to the definition used by metallurgists. The 170% elongation reported by Wakai et al. [44] on 3Y-TZP has been considered as evidence of ceramic superplasticity in the ceramic materials. 3Y-TZP, termed as 'ceramic steel' [46, 47], is now considered to be the model ceramic system. The fine grade size leads to a very dense, non-porous ceramic with excellent mechanical strength, corrosion resistance, impact toughness, thermal shock resistance and very low thermal conductivity. Due to its characteristics Y-TZP is used in wear parts, cutting tools and thermal barrier coatings.

Also, electrical properties of 3Y-TZP are very interesting. At moderate temperatures below 970 K the grain interior of Y-TZP has higher conductivity [47, 48] than that of fully (YSZ) or partially stabilized (PSZ) zirconia [50]. However, the total conductivity of Y-TZP is lower due to the high contribution of grain boundary resistivity, known as the blocking effect [47, 49]. It was found that addition of Al_2O_3 leads considerable reduction of the blocking effect [50].

4.1. Defect structure of YSZ

The defect reactions in the yttria-stabilized zirconia can be written as:

$$Y_2O_3 \rightarrow \quad 2Y'_{Zr} + V_O^{\bullet\bullet} + 3\, O_O^x \tag{16}$$

$$O_O^x \Leftrightarrow V_O^{\bullet\bullet} + 2\, e' + \frac{1}{2}\, O_2 \tag{17}$$

$$nil \Leftrightarrow e' + h^{\bullet} \tag{18}$$

The majority defect oxygen in yttria-stabilized zirconia are oxygen vacancies $V_O^{\bullet\bullet}$ and yttrium ions Y^{3+} (Y'_{Zr} using defect notation) occupying zirconium positions the electroneutrality conditions is given by:

$$2\left[V_O^{\bullet\bullet}\right] = \left[Y'_{Zr}\right] \tag{19}$$

Ionic conductivity of $ZrO_2 + 10$ mol% Y_2O_3, termed as 10YSZ resulting from the Eq. (19) is illustrated in **Figure 8** [51].

Combining Eqs. (16)–(19) we can determine concentration of both electronic defects:
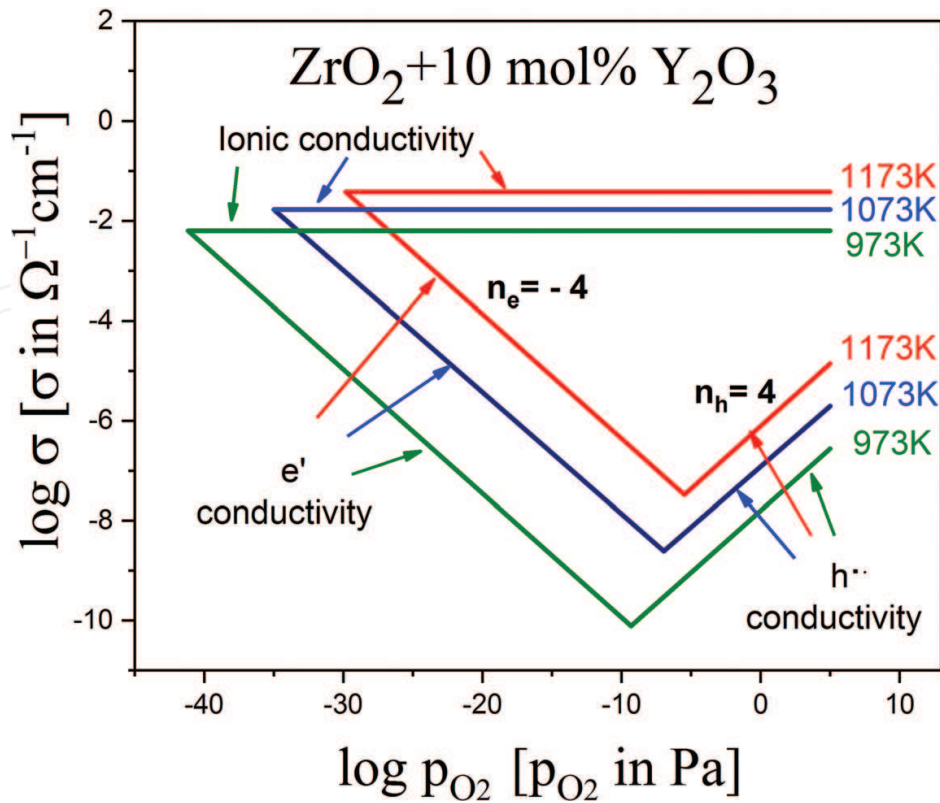
Figure 8. Both ionic and electronic components of the electrical conductivity of yttria-stabilized zirconia (10YSZ) in the range 973–1173 K as a function of p_{O_2}, according to Weppner [51].
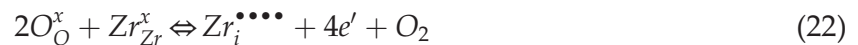
$$[e'] = \left\{ \frac{2K_V}{[Y'_{Zr}]} \right\}^{1/2} p_{O_2}^{-1/4} \tag{20}$$

and

$$[h^\bullet] = \left\{ \frac{K_i^2 [Y'_{Zr}]}{2K_V} \right\}^{1/2} p_{O_2}^{1/4} \tag{21}$$

where K_V and K_i are equilibrium constants of reactions (17) and (18), respectively. Dependences of electrons and electron holes conductivities are presented in **Figure 8**.

The possible minority defects are: zirconium interstitials $Zr_i^{\bullet\bullet\bullet\bullet}$ and zirconium vacancies V_{Zr}''''. They occupy positions in zirconium sublattice and form according to the following reactions:

$$2O_O^x + Zr_{Zr}^x \Leftrightarrow Zr_i^{\bullet\bullet\bullet\bullet} + 4e' + O_2 \tag{22}$$

and

$$O_2 + 4e' \Leftrightarrow 2O_O^x + V_{Zr}'''' \tag{23}$$

Applying the mass action law to reactions (22) and (23) gives:

$$\left[Zr_i^{\bullet\bullet\bullet\bullet}\right] = K_{22}[e']^{-4}p_{O_2}^{-1} \tag{24}$$

and

$$\left[V_{Zr}''''\right] = K_{23}[e']^{4}p_{O_2} \tag{25}$$

where K_{22} and K_{23} are the equilibrium constants of reactions (22) and (23), respectively.

4.2. Creep of single crystalline zirconia

Marcartney et al. [52] studied creep of single crystal zirconia stabilized with 12 mol% CaO within 1623–1723 K. They observed considerable climb and glide formation. Dominguez-Rodriguez et al. [53–56] examined cubic YSZ (9.4–18 mol% Y_2O_3) single crystals. The determined activation energies of the deformation process were 646.4; 800.8 and 944.7 kJ/mol for 9.4, 12 and 18 mol% of yttria, respectively. Lankford [57] studied the deformation of two single crystals of YSZ containing 2.8 and 12 mol% Y_2O_3.The temperature range of the experiments was 296–1423 K. The plastic flow with rapid decrease in strength with increasing temperature was observed. The deformation was attributed to dislocation activity alone. Corman [58] examined the creep of single crystal 9.5 mol% yttria partially stabilized zirconia, within temperature range 1923–2123 K and stress from 12.5 to 100 MPa.

The stress exponent, m, and activation energy Q (Eq. (1)) were m = 4 and Q = 436 kJ/mol. This value is close to the lattice diffusion of Zr (418 kJ/mol). So, he concluded that cation diffusion is controlled the process deformation.

4.3. Creep of polycrystalline zirconia

The dependence of steady state creep rate, $\dot{\varepsilon}$; on stress, σ; temperature, T and grain size, d of polycrystalline zirconia is given by a general relationship of the form:

$$\dot{\varepsilon} = \frac{ADGb}{kT}\left(\frac{b}{d}\right)^{p}\left(\frac{\sigma}{G}\right)^{m} \tag{26}$$

where A is a dimensionless constant, G is the shear modulus, b is the Burgers vector, k is Boltzmann's constant, p and m are constants termed the inverse grain size and stress exponent, respectively and D is the appropriate diffusion coefficient given by:

$$D = D_o \, exp\left(-\frac{Q}{RT}\right) \tag{27}$$

where D_o is a frequency factor, Q is the appropriate activation energy and R is the gas constant.

Creep of polycrystalline zirconia was recently intensively studied. The subjects of interest were cubic stabilized zirconia, CSZ [59–64], partial stabilized zirconia, PSZ [65–67] as well as tetragonal zirconia polycrystals, TZP [44, 68–73].

St Jacques and Angers [59] examined zirconia stabilized with 18 mol% CaO in the temperatre range 1470–1670 K and stress between 3.5 and 27.5 MPa. The parameter m in Eq. (26) was equal to 1, which suggested diffusionally controlled creep. The detailed study by Dimos and Kohlstedt [60] on a cubic 25YSZ indicated that the creep is controlled by the Nabarro-Herring diffusion mechanism with parameters m ≈ 1 and p ≈ 2. Wakai et al. [61, 63] reported that a stress exponent m ≈ 2 in an 8YSZ. Sharif et al. [64] studying a static grain growth claimed that cubic zirconia is prone to extensive grain growth.

Evans [66] studied deformation of yttria- and scandia- partially stabilized zirconia, PSZ (1436 < T < 1808 K; 4.1 < σ < 7.1 MPa). The activation energies were 373 and 360 kJ/mol for scandia and yttria, respectively, the parameter p = 2 was found, the parameter m was 1.5 for scandia stabilized zirconia and it assumed two values m = 1 and m = 6 for yttria. Seltzer, and Talty [67] studied Y-PSZ at high temperatures (up to 2270 K), they found m = 1.5 for fine-grained samples (d varied from 15 to 20 μm) and activation energy was 531 kJ/mol. Chevalier et al. [68] studied PSZ materials stabilized by MgO, they concluded that cavitations and microcracking by grain boundary sliding have been identified as the main creep mechanisms.

Wakai et al. [44] examined creep of 3Y-TZP within temperature range of 1423–1723 K. The stress exponents m = 1.5 at 1423 K and gradually increased with temperature reaching value m = 1.9 at 1723 K. The activation energy was 586 kJ/mol. Nauer and Carry [69] investigated the creep behavior TZP containing 2, 3 and 4 mol% Y_2O_3. At lower stresses (σ < 10 MPa) the parameters were: m = 2.4 and p = 1 and activation energy Q = 590 kJ/mol. At higher stresses ca. 100 MPa, the parameter m = 1. Authors proposed two different deformation regimes: an interface reaction controlled creep at low stresses and a grain boundary diffusion controlled creep at high stresses. Lakki et al. [70] studied 2Y-TZP material using two techniques the creep and the internal friction (it consists on applying a cyclic stress σ = $σ_o$ cos (ωt) to a sample and measuring its response in the form of strain, ε). Both techniques provide at low stresses (< 15 MPa) close values of the activation energies and lead to conclusion that grain boundary sliding is the main deformation mechanism. Owen and Chokshi [71] and Chokshi [72] investigated 3Y-TZP. The experimental data over a wide range of stresses revealed a transition in stress exponent. Deformation at low and high stress regions was associated with m ≈ 3, p ≈ 1 and m ≈ 2, p ≈ 3, respectively. The activation energy was Q ≈ 550 kJ/mol for both regions. Authors postulated that the interface reaction is controlled at low stress region and the grain boundary sliding at high stress region. Ghosh et al. [73] examined effect of silica additions on creep behavior of 3Y-TZP. The determined results were verified by tracer diffusion measurements. The creep data at high stresses are consisted with Coble diffusion and creep at lower stresses is attributed to interface-controlled diffusion mechanism. Addition of silica has only minor effect on both grain boundary and lattice diffusion. Ghost and Chokshi [74] studied the creep of nanocrystalline 3Y-TZP who obtained results indicating the same deformation mechanism as for micro-sized materials. Liu et al. [75] examined creep behavior of zirconia stabilized with 2.5 mol%. They postulated the grain boundary sliding accompanied by intergranular dislocation due to existence of amorphous phases.

5. Summary

The emphasis of this review was to compile existing data in the creep behavior of two types of oxides: iron-row group $M_{1-y}O$ (M = Ni, Co, Fe) which properties are strongly related with the oxygen partial pressure (p_{O_2}) dependent departure from stoichiometry (y) and superionic ZrO_2-based materials. Two different approaches to creep methodology are used. In case of the transition metal oxides such as $M_{1-y}O$ the creep experiments required determination of the rate deformation ($\dot{\varepsilon}$) as a function σ, T, p_{O_2} and grain size (d) for polycrystalline materials. On the other hand, the oxide superionics such as stabilized zirconia concentration of ionic defects ($\left[V_O^{\bullet\bullet} \right]$) is fixed by the amount used stabilizer (usually Y_2O_3). Electronic defects (e′ and h$^\bullet$) play role only in the extremely reduced or oxidizing conditions (usually very hard to achieve experimentally). Therefore, the creep rate is studied as a function σ, T and d in case of the polycrystals.

From this review several general trends in creep behavior emerge. Deformation of single crystals is typically controlled by dislocation glide on the most favorable slip system. On the other hand, deformation of polycrystalline oxides is controlled by diffusion of the slowest species along the fastest path, such as through the lattice, along grain boundaries or through a second phase formed at the grain boundaries. Dislocations play a more or less important role depending on the specific oxide.

Steady state creep of $M_{1-y}O$ appears to be controlled by oxygen diffusion through either oxygen vacancies or interstitials. On the other hand in case of stabilized zirconia it is controlled by cation diffusion (Zr^{4+} or Y^{3+}). In any cases diffusion, involving both lattice and grain boundary data are needed to verification of proposed mechanisms. Recently used secondary ion mass spectrometry (SIMS) is suitable for this purpose [73, 76–78].

Acknowledgements

Author details

Krystyna Schneider* and Mieczyslaw Rekas

*Address all correspondence to: kryschna@agh.edu.pl

AGH, University of Science and Technology, Krakow, Poland

References

[1] Ashby M. Materials. Oxford: Elsevier; 2014. p. 336

[2] Bretheau T, Castaing J, Rabier J, Veyssiere P. Dislocations motion and high temperature plasticity of binary and ternary oxides. Advances in Physics. 1979;**28**:835

[3] Philibert J. Creep and diffusion. Solid State Ionics. 1984;**12**:321-336

[4] Rekas M, Mrowec S. On defect clustering in the wustite phase. Solid State Ionics. 1987;**22**: 185-197

[5] Nowotny J, Rekas M. Defect structure and thermodynamic properties of the wustite phase ($Fe_{1-y}O$). Journal of the American Ceramic Society. 1989;**72**:1221-1228

[6] Dickmann R. Cobaltous oxide point defect structure and non-stoichiometry, electrical conductivity, cobalt tracer diffusion. The Journal of Physical Chemistry. (Munich. 1977;**107**:189-210

[7] Nowotny J, Rekas M. Seebeck effect of undoped and Cr-doped NiO. Solid State Ionics. 1984;**12**:253-261

[8] Kröger FA, Vink HJ. In: Seitz F, Turnbull D, editors. Solid State Physics. Vol. 3. New York: Academic Press; 1956. p. 307

[9] Bransky I, Tallan NM. High temperature defect structure and electrical properties of NiO. The Journal of Chemical Physics. 1968;**49**:1243-1249

[10] Farhi R, Petot-Ervas G. Thermodynamic study of point defects in single crystalline nickel oxide. Analysis of experimental results. Journal of Physics and Chemistry of Solids. 1978;**39**:1175-1179

[11] Domingues-Rodrigueez A, Castaing J, Philibert J. Plastic deformation of pure and doped Nio single crystals. Materials Science and Engineering. 1977;**27**:217-223

[12] Carrera-Caño J, Domingues-Rodrigueez A, Marquez R, Castaing J, Philibert J. Point defects and high-temperature creep of non-stoichiometric NaCl-type oxide single crystals. I, NiO. Philosophical Magazine A. 1982;**46**:397-407

[13] Jimenez-Melendo M, Cabrera-Cano J, Dominguez-Rodriguez A, Castaing J. Pure diffusional creep of NiO polycrystals. The Journal of Physical Chemistry Letters. 1983;**44**: L-339-L-343

[14] Krishinamachri V, Notis MR. High temperature deformation of polycrystalline NiO and CoO. Acta Metallurgica (pre 1990). 1977;**25**:1307

[15] Dubois C, Monty C, Philibert J. Oxygen self- diffusion in NiO single crystals. Philosophical Magazine A. 1982;**46**:419-433

[16] Dubois C, Monty C, Philibert J. Influence of oxygen pressure on oxygen self-diffusion in NiO. Solid State Ionics. 1984;**12**:75-78

[17] Choi JS, Moore WJ. Diffusion of nickel in single crystals of nickel oxide. The Journal of Physical Chemistry. 1962;**66**:1308-1311

[18] Lindner RL, Akerstro A. Diffusion of nickel-63 (NiO). Discussions of the Faraday Society. 1957;**23**:133-136

[19] O'Keeffe M, Moore WJ. Diffusion of oxygen in single crystal of nickel oxide. The Journal of Physical Chemistry. 1961;**65**:1435-1439

[20] Nowotny J, Rekas M, et al. Journal of the American Ceramic Society. 1989;**72**:1199-1207

[21] Stoneham AM, Tomlison SM, Catlow CRA, Harding JH. Clustering of defects. In: Adles D, Fritsche H, Ovshinsky SR, editors. Physics of Disordered Materials. New York: Plenum Press; 1985. p. 243-252

[22] Nowotny J, Rekas M. Defect structure of cobalt monoxide. II. The Debye-Hückel Model. Journal of the American Ceramic Society. 1989;**72**:1207-1214

[23] Nowotny J, Rekas M. Defect structure of cobalt monoxide. III. The cluster model. Journal of the American Ceramic Society. 1989;**72**:1215-1220

[24] Clauer AH, Selzer MS, Wilcox BA. Creep of CoO single-crystals. Journal of Materials Science. 1971;**4**:1379-1388

[25] Krishinamachri V, Jones JT. Compressive creep of CoO single crystals. Journal of the American Ceramic Society. 1974;**57**:506-507

[26] Nehring VW, Smyth JR, McGee TD. Compressive creep of CoO single crystals. Journal of the American Ceramic Society. 1974;**60**:328-332

[27] Routbort JL. The stoichiometry dependence of the deformation of $Co_{1-\delta}O$. Acta Metallurgica. 1982;**30**:663-671

[28] Dominguez-Rodriguez A, Sanchez M, Marquez R, Castaing J, Monty C, Philibert J. Point defects and high-temperature creep of non-stoichiometric NaCl-type oxide single crystals. II CoO. Philosophical Magazine A. 1982;**46**:411-418

[29] Darken LS, Gurry RW. The system iron-oxygen II Equilibrium and thermo-dynamics of liquid oxide and other phases. Journal of the American Chemical Society. 1946;**68**:798-812

[30] Roth WL. Defects in the crystals and magnetic structure of ferrous oxide. Acta Crystallographica. 1960;**13**:140-149

[31] Nowotny J, Rekas M, Wierzbicka M. Defect structure and electrical properties of the wustite phase. Zeitschrift für Physikalische Chemie. 1982;**131**:191-198

[32] Koch FB, Cohen JB. Defect structure of $Fe_{1-y}O$. Acta Crystallographica Section B. 1969;**25**:275-287

[33] Cheetham AK, Fender BEF, Taylor RI. High temperature neutron diffraction study of $Fe_{1-y}O$. Proceedings of the Physical Society. London, Solid State Physics. 1971;**4**:2160-2165

[34] Battle PD, Cheetham AK. The magnetic structure in non-stoichiometric ferrous oxide. Journal of Physics C. 1979;**12**:337-345

[35] Catlow CRA. Defect clustering in non-stoichiometric oxides. In: Sørensen T, editor. Nonstoichiometric Oxides. New York: Academic Press; 1981. p. 61-98

[36] Stoneham AM, Tomlinson SM, Catlow CRA, Hardings JH. Defect clustering in rock-salt structured transition metal oxides. In: Simkovich G, Stubican VS, editors. Transport in Non-Stoichiometric Compounds. New York: Plenum Press; 1985. p. 243-252

[37] Ilschner B, Reppich B, Riecke E. High-temperature steady-state creep and atomic disorder in iron^{II} oxide. Discussions of the Faraday Society. 1964;**38**:243-250

[38] Jolles E, Monty C. High temperature creep of $Fe_{1-x}O$. Philosophical Magazine A. 1991;**64**:765-775

[39] Badwal SPS, Bannister MJ, Hannik RHJ, editors. Science and Technology of Zirconia V. Basel: Technocomic Publ. Comp.; 1993

[40] Somiya S, Yamamoto N, Yanagida H, editors. Science and Technology of Zirconia III. Westerville, OH (USA): American Ceramic Society Inc; 1988

[41] Claussen N, Ruhle M, Heuer AH, editors. Science and Technology of Zirconia, II. Columbus, OH (USA): American Ceramic Society, Inc; 1983

[42] Kisi E. Zirconia Engineering Ceramics. Switzerland: Trans.Tech. Publ. Ltd; 1998

[43] Garvie RC, Nicholson PS. Structure and thermo-mechanical properties of partially stabilized zirconia in the $CaO-ZrO_2$ system. Journal of the American Ceramic Society. 1972;**55**:152-157

[44] Wakai F, Sakaguchi S, Matsuno Y. Superplasticity of yttia-stabilized tetragonal ZrO_2 polyctrystals. Advanced Ceramic Materials. 1986;**1**:259-263

[45] Carry C. In: Kobayashi M, Wakai F, editors. Proceedings of the MRS International Meeting on Advanced Materials, Pittsburgh, PA (USA). 1989;**7**:199-215

[46] Garvie RC, Hannik RH, Pacoe RT. Ceramic steel. Nature. 1975;**258**:703-704

[47] Badwal SPS. Yttria tetragonal zirconia polycrystalline electrolytes for solid state electrochemical cells. Applied Physics A. 1990;**50**:449-462

[48] Badwal SPS, Drennan J. Grain boundary resistivity in Y-TZP materials as a function of thermal history. Journal of Materials Science. 1989;**24**:88-96

[49] Meyer D, Eisele U, Satet R, Rödel J. Codoping of zirconia with yttria and Scandia. Scripta Materialia. 2008;**58**:215-218

[50] Obal K, Brylewski T, Pedzich Z, Rekas M. Modification of yttria-doped tetragonal zirconia polycrystal ceramics. International Journal of Electrochemical Science. 2012;**7**: 6831-6845

[51] Weppner W. Electrochemical transient investigations of the diffusion and concentration of electrons in yttria sabilized zirconia-solid electrolytes. Zeitschrift für Naturforschung. 1976;**31a**:1336-1343

[52] Mecartney ML, Donlon WT, Heuer AH. Plastic deformation in CaO stabilized ZrO_2 (CSZ). Journal of Materials Science. 1980;**15**:1063-1065

[53] Dominguez-Rodriguez A, Lagerloff KPD, Heuer AH. Plastic deformation and solid-solution hardening of Y_2O_3-stabilized ZrO_2. Journal of the American Ceramic Society. 1986;**69**:281-284

[54] Martinez-Fernandez J, Jimenez-Melendo M, Dominguez-Rodriguez AA. High temperature creep of yttria-stabilized zirconia single crystals. Journal of the American Ceramic Society. 1990;**73**:2452

[55] Dominguez-Rodriguez A, Jemenez-Melendo M, Casting J. Plasticity of zirconia. In: Bradt RC, Brookes CA, Routbort JL, editors. Deformation of Ceramics. New York: Plenum Press; 1995. p. 31-41

[56] Gomez-Garcia D, Martinez-Fernandez J, Dominguez-Rodriguez A, Casting J. Mechanizm of high-temperature creep of full stabilized zirconia single crystals as a function of the yttria content. Journal of the American Ceramic Society. 1997;**80**:1668-1672

[57] Lankford J. Deformation and fracture of Yttria-stabilized zirconia single crystals. Journal of Materials Science. 1986;**21**:1981-1989

[58] Corman GS, High-temperature creep of yttria-stabilized zirconia single crystals. G.E. Research and Development, Technical Information Series. 1989. Ceramics Laboratory, Schenectady NY (USA) #89CRD084

[59] St Jacques RG, Angers R. Creep of CaO-Stabilized ZrO_2. Journal of the American Ceramic Society. 1972;**55**:571-574

[60] Dimos D, Kohlstedt DL. Diffusional creep and kinetic demixing in yttria-stabilized zirconia. Journal of the American Ceramic Society. 1987;**70**:531-536

[61] Chen I-W, Xue LA. Development of superplastic structural ceramics. Journal of the American Ceramic Society. 1990;**73**:2585-2609

[62] Wakai F, Nagano T. Effecxt of solute ion and grain size on superplasticity of ZrO_2 polycrystals. Journal of Materials Science. 1991;**26**:241-247

[63] Wakai F. Step model of solution-precopitation creep. Acta Metallurgica et Materialia. 1994;**42**:1163-1172

[64] Sharif AA, Imamura PM, Michell TE, Mecartney ML. Control of grain growth using intergranular silicate phase in cubic yttria-stabilized zirconia. Acta Materialia. 1998;**6**:3863-3872

[65] Sudhir B, Chokshi AH. Compression creep characteristics of 8 mol% - yttria-stabilized zirconia. Journal of the American Ceramic Society. 2001;**84**:2625-2632

[66] Evans PE. Creep in yttria- and scandia-stabilized zirconia. Journal of the American Ceramic Society. 1970;**53**:365-369

[67] Seltzer MS, Talty PK. High temperature creep of Y_2O_3 – stabilized ZrO_2. Journal of the American Ceramic Society. 1975;**58**:124-130

[68] Chevalier J, Olagon C, Fantzyyi G, Gros H. Creep behavior of alumina, zirconia and zirconia-toughened alumina. Journal of the European Ceramic Society. 1997;**17**:859-864

[69] Nauer M, Carry C. Creep parameters of yttria doped zirconia materials and superplasticity deformation mechanisms. Scripta Metallurgica et Materialia. 1990;**24**:1459-1463

[70] Lakki A, Schaller R, Nauer M, Carry C. High temperature siperplastic creep and internal friction of yttria doped zirconia polycrystals. Acta Metallurgica et Materialia. 1993;**41**: 2845-2853

[71] Owen DM, Hokshi AH. The high temperature mechanical characteristics of super plastic 3 mol% yttria stabilized zirconia. Acta Materialia. 1998;**46**:667-679

[72] Chokshi AH. The role of diffusion creep in the superplastic deformation of 3 mol% yttria stabilized tetragonal zirconia. Scripta Materialia. 2000;**42**:241-248

[73] Ghosh S, Kilo M, Borchardt G, Chokshi AH. Diffusion and creep in silica-doped tetragonal zirconia. Journal of the American Ceramic Society. 2009;**92**:3004-3013

[74] Ghosh S, Chokshi AH. Creep in nanocrystalline zirconia. Scripta Materialia. 2014;**86**:13-16

[75] Liu E, Wang H, Xiao G, Yuan G, Shu X. Creep-related micromechanical behavior of zirconia-based ceramics investigated by nanoindentation. Ceramics International. 2015. DOI: 10.1016/j.ceramint 2015.06.136

[76] Bak T, Nowotny J, Prince K, Rekas M, Sorrell CC. Grain boundary diffusion of magnesium in zirconia. Journal of the American Ceramic Society. 2002;**85**:2244-2250

[77] Swaroop S, Kilo M, Argirusis C, Borchardt G, Chokshi AH. Lattice and grain boundary diffusion of cations in 3Y-TZP. Analyzed using SIMS. Acta Materialia. 2005;**53**:4975-4985

[78] Kowalski K, Obal K, Pedzich Z, Schneider K, Rekas M. Lattice and grain boundary diffusion of Al in tetragonal yttria-stabilized zirconia polycrystalline ceramics (3Y-TZP). Analyzed using SIMS. Journal of the American Ceramic Society. 2014;**97**:3123-3127